Magnetic Resonance Angiography in the Diagnosis of Cerebral Arteriovenous Malformation and Dural Arteriovenous Fistulas: Comparison of Time-Resolved Magnetic Resonance Angiography and Three Dimensional Time-of-Flight Magnetic Resonance Angiography

Yu-Ching Cheng,[1] Hung-Chieh Chen,[1] Chen-Hao Wu,[1,2,*] Yi-Ying Wu,[1] Ming-His Sun,[3] Wen-Hsien Chen,[1] Jyh-Wen Chai,[1] and Clayton Chi-Chang Chen[1]

[1]Department of Radiology, Taichung Veterans General Hospital, Taichung, Taiwan
[2]Department of Medical Imaging and Radiological Sciences, Central Taiwan University of Science and Technology, Taichung, Taiwan
[3]Department of Neurosurgery, Taichung Veterans General Hospital, Taichung, Taiwan

[*]*Corresponding author*: Chen-Hao Wu, Department of Radiology, Taichung Veterans General Hospital, Taichung, Taiwan. Fax: +886-423595046, E-mail: chenhaowu@vghtc.gov.tw

Abstract

Background: Traditional digital subtraction angiography (DSA) is currently the gold standard diagnostic method for the diagnosis and evaluation of cerebral arteriovenous malformation (AVM) and dural arteriovenous fistulas (dAVF).

Objectives: The aim of this study was to analyze different less invasive magnetic resonance angiography (MRA) images, time-resolved MRA (TR-MRA) and three-dimensional time-of-flight MRA (3D TOF MRA) to identify their diagnostic accuracy and to determine which approach is most similar to DSA.

Patients and Methods: A total of 41 patients with AVM and dAVF at their initial evaluation or follow-up after treatment were recruited in this study. We applied time-resolved angiography using keyhole (4D-TRAK) MRA to perform TR-MRA and 3D TOF MRA examinations simultaneously followed by DSA, which was considered as a standard reference. Two experienced neuroradiologists reviewed the images to compare the diagnostic accuracy, arterial feeder and venous drainage between these two MRA images. Inter-observer agreement for different MRA images was assessed by Kappa coefficient and the differences of diagnostic accuracy between MRA images were evaluated by the Wilcoxon rank sum test.

Results: Almost all vascular lesions (92.68%) were correctly diagnosed using 4D-TRAK MRA. However, 3D TOF MRA only diagnosed 26 patients (63.41%) accurately. There were statistically significant differences regarding lesion diagnostic accuracy (P = 0.008) and venous drainage identification (P < 0.0001) between 4D-TRAK MRA and 3D TOF MRA. The results indicate that 4D-TRAK MRA is superior to 3D TOF MRA in the assessment of lesions.

Conclusion: Compared with 3D TOF MRA, 4D-TRAK MRA proved to be a more reliable screening modality and follow-up method for the diagnosis of cerebral AVM and dAVF.

Keywords: 4D-TRAK MRA, 3D TOF MRA, Cerebral Arteriovenous Malformation, Cerebral Dural Arteriovenous Fistulas

1. Background

Several imaging modalities are used for the diagnosis or post-treatment follow-up of cerebral vascular lesions. These methods include traditional digital subtraction angiography (DSA), computed tomographic angiography (CTA) and magnetic resonance angiography (MRA) (1-6). The traditional catheter-based intracranial DSA is still the gold standard for the diagnosis of cerebral vascular lesions, such as arteriovenous malformations (AVM) and dural arteriovenous fistulas (dAVF) (5, 7). However, the potential risks of DSA, such as neurological procedural complications or ionizing radiation exposure, may lead to unwanted morbidity and mortality (8, 9). Alternatively, CTA and MRA are becoming more popular. Due to the high ion-izing radiation in CTA examinations (3, 10) and a higher possibility of an anaphylactic reaction to the CT contrast medium in patients (11), MRA is gaining importance for use in cerebral vascular lesions and has become a potential alternative for both diagnosis and follow-up.

Several different MRA methods have been applied in clinical use as less invasive, safer alternatives to DSA. Three-dimensional time-of-flight MRA (3D TOF MRA), conventional contrast-enhanced MRA (CE-MRA), and time-resolved MR angiography (TR-MRA) have been gaining more and more clinical acceptance in the evaluation of cerebral vascular lesions (12, 13). Among these MRA techniques, 3D TOF MRA is used for intracranial vascular evaluation without contrast medium injection. However, it is

limited by its lack of hemodynamic information (13). Although CE-MRA has good spatial resolution, it also fails to provide hemodynamic information (14). Therefore, it is important to develop an MRA with hemodynamic information that resembles traditional DSA. For this reason, TR-MRA technique has been developed (14).

TR-MRA is a new technique for improving temporal resolution. Compared with CE-MRA, TR-MRA applies parallel imaging (including both in-plane and through-plane), partial Fourier data sampling, and a special k-space sampling method to greatly reduce acquisition times and preserve adequate spatial resolution (15-18). Several vendors have provided new techniques, including 4D time-resolved angiography using keyhole (4D-TRAK) (19), time-resolved imaging with stochastic trajectories (TWIST) (20), time-resolved echo-shared angiography technique (TREAT) (21), and time-resolved imaging of contrast kinetics (TRICKS) (14). The 4D-TRAK MRA combines contrast-enhanced timing-robust angiography (CENTRA) (22) and the keyhole method (19) to improve temporal resolution without compromising spatial resolution of the dynamic images (21). Hemodynamic information obtained by 4D-TRAK MRA has sequential arterial and venous phase images, much as the traditional DSA (23-25). Thus, the images acquired with the aid of 4D-TRAK MRA are conducive to improving the diagnostic accuracy of cerebral vascular lesions.

Despite the fact that DSA is still irreplaceable in the diagnosis of cerebral vascular lesions, we wanted to find a more reliable less invasive imaging tool for the diagnosis of cerebral vascular lesions. Among several MRA modalities, 3D TOF MRA is currently routinely performed at most hospitals (2, 26, 27); whereas, 4D-TRAK MRA is still not widely applied. Although, recently, Wu and Li (28) have revealed that 4D-TRAK MRA could provide a similar diagnostic accuracy rate for evaluation of cerebral aneurysms (CAs) and a better characterization of morphology for larger CAs compared to 3D TOF MRA, it still remains unclear which method performs better in terms of diagnostic accuracy for cerebral AVM and dAVF.

2. Objectives

In this study, we used 4D-TRAK MRA and 3D TOF MRA to diagnose cerebral AVM and dAVF and employed DSA images as standard references. By studying the two protocols, we attempted to determine whether any differences in interobserver agreement exist between the two techniques and which achieves more accurate diagnoses.

3. Patients and Methods

3.1. Participants

From January 2010 to December 2012, people who had been diagnosed or underwent MRI for post-treatment follow-up of cerebral vascular lesions were recruited in our study. They received both 4D TRAK MRA and 3D TOF MRA at the same time. The patients then received DSA as a standard reference for the final diagnosis. The interval between DSA and MRA was limited within one month. Patients who did not fit these criteria were excluded. Treatment methods included endovascular treatment, gamma knife radiosurgery, and surgical intervention. Endovascular treatment included transarterial embolization using stainless steel coils, glue (N-butyl cyanoacrylate, NBCA) or EVOH (Onyx, Micro Therapeutics, Irvine, CA) (29). Before enrollment of the patients into this study, written informed consent was obtained from all subjects. The images were retrospectively analyzed. This study was approved by the institutional review board of Taichung veterans general hospital, Republic of China.

3.2. MRI Data Acquisition

Participants were scanned on a 3T MR scanner (Achieva, Philips Healthcare, Best, the Netherlands) with an eight-channel SENSE-capable head coil. Head movement was restricted with expandable foam cushions. The slice orientation of all axial images was performed in parallel to the line connecting the anterior and posterior commissure on the mid-sagittal localizer. Basic MR images were as follows: axial T1-weighted spin echo images (TR, 500 ms; TE, 10 ms) and axial T2-weighted fast spin echo images (TR, 3200 ms; TE, 115 ms). Axial and coronal post-contrast enhanced T1-weighted spin echo images were acquired after 4D-TRAK MRA acquisition.

3.3. MR Angiography

3D TOF-MRA was performed with five axial slabs of 180 slices, each with a 0.8-mm thickness that spanned and covered the whole brain. The sequence parameters were as follow: TR, 23 ms; TE, 1.86 ms; flip angle, 18°; field of view (FOV), $200 \times 200 \times 144$ mm^3. These settings resulted in the acquisition of 3D data with $0.5 \times 0.7 \times 0.8$ mm^3 voxels in 5 minutes 40 seconds. The MRA was processed with maximum intensity projection (MIP) reconstructed in 180 degrees rotation in two directions: head to foot and left to right.

TR-MRA was performed using a sequential T1-weighted 4D-TRAK MRA sequence. The following parameters were constant in all examinations: TR, 3.3 ms; TE, 1.02 ms; flip angle, 20°; FOV, $230 \times 246 \times 160$ mm^3; parallel imaging with

an acceleration factor of 8 (phase encoding, 4; section encoding, 2); and half-Fourier imaging with 30% k-space reduction. The intravenous injection of 0.1 mL/kg contrast agent (gadobutrol, 1 mmol/mL; Gadovist 1.0; Bayer Schering Pharma, Bayer Vital, Leverkusen, Germany) with a flow rate of 3 mL/s was followed by a 20 mL saline flush delivered with an automated power injector. We achieved a total of 30 dynamic acquisitions, 1.6 seconds per volume combined with a reference scan of 5.5 seconds for a total acquisition time of 53.6 seconds and a spatial resolution at acquisition of $0.8 \times 1.3 \times 2\,mm^3$ after interpolation in a voxel size of $0.77 \times 0.77 \times 1\,mm^3$. For 4D-TRAK MRA visualization, native or subtracted data (4,600 images) were used by a local medical software called MR project (medical research project) dedicated to analyzing 4D with MIP ray tracing. The software enabled enlargement of regions of interest in any 3D direction with the possibility of viewing progress of contrast injection, which is in contrast to the simple dynamic series of MIP images generated in sagittal, coronal, and axial views.

3.4. Conventional Angiography

Diagnostic biplanar intra-arterial DSA (Allura Xper FD 20/20; Philips Medical Systems, Best, the Netherlands) was performed by a trained neuroradiologist with a 4.1Fr. catheter that was navigated into the internal carotid, external carotid, and both vertebral arteries via the transfemoral route. The images were obtained after power injection of 5 - 8 mL of iopromide (Ultravist; Bayer Healthcare). Frame rates were 6 frame/s in the arterial phase and 4 frame/s in the venous phase.

3.5. Qualitative Analysis

Two neuroradiologists (7 and 13 years of experience in neuroimaging) with no knowledge of the DSA results interpreted 4D-TRAK MRA data in 3 MIP-subtracted orthogonal images (sagittal, coronal, and axial) and 3D TOF MRA images in a random order on a PACS system. The DSA images were reviewed by a senior neuroradiologist (17 years of experience in neuroangiography) without knowledge of the MRA findings. Both groups were blinded to the clinical history. The overall diagnostic accuracy index was scored according to a 3-point grading system comparing with DSA: score of 2, "adequate" for diagnosis (depiction of feeding arteries and draining veins was possible, minor artifacts might be present but did not interfere with image interpretation); score of 1, "questionable" for diagnosis (depiction of feeding arteries and draining veins was impaired by artifacts and/or inadequate temporal resolution); score of 0, "nondiagnostic" (image quality was not sufficient for diagnosing feeding arteries and draining veins because of

artifacts and/or poor temporal resolution). Conflicts between observers were reviewed by both readers to reach a consensus (30). The 3D data were displayed with all regions visible. The software allowed for enlargement of regions of special interest in any given spatial orientation. Diagnostic parameters were analyzed based on the following three criteria: diagnostic accuracy, depiction of arterial feeders and depiction of venous drainage. The diagnostic accuracy defined as the diagnosis made by MRA examinations was the same as DSA.

3.6. Statistical Analysis

Kappa coefficient was used to calculate the interobserver agreement (between two readers for 3D TOF MRA and 4D-TRAK MRA). The diagnostic accuracy and depiction of arterial feeders and venous drainage in 4D-TRAK MRA and 3D TOF MRA were individually determined by calculating the κ coefficient ($\kappa < 0.20$, poor; $\kappa = 0.21 - 0.40$, fair; $\kappa = 0.41 - 0.60$, moderate; $\kappa = 0.61 - 0.80$, good; $\kappa = 0.81 - 0.90$, very good; and $\kappa > 0.90$, excellent agreement). The nonparametric Wilcoxon rank sum test was applied to compare the diagnostic accuracy between 4D-TRAK MRA and 3D TOF MRA, and a P value < 0.05 was considered as statistically significant. Statistical comparisons were performed using SPSS software version 17 (SPSS Inc., Chicago, Illinois).

4. Results

4.1. Demographic Data

A total of 41 patients (15 women and 26 men) whose ages ranged from 13 to 82 years (mean age, 41.7 years) with cerebral vascular lesions, including 32 AVM patients and nine dAVF patients, were recruited and definitively diagnosed by DSA. Of these patients, 17 were initially diagnosed with previously unknown cerebral vascular lesions, and 24 patients were followed up after treatment. The demographic data of the patients are listed in Table 1.

4.2. Summary of Scoring Based on a 3-Point Grading System

Table 2 provides a summary of the scoring for diagnostic accuracy, arterial feeder, and venous drainage. Regarding the diagnostic accuracy, including lesion location and fistula point, 38 patients (92.68%) were correctly diagnosed using 4D-TRAK MRA, and three were poorly diagnosed (7.32%). However, 3D TOF MRA only accurately diagnosed 26 (63.41%) patients, equivocally diagnosed six patients (14.63%), and poorly diagnosed nine patients (21.95%). As for arterial feeder, 4D-TRAK MRA and 3D TOF MRA showed well-recognized images in 30 patients (73.17%) and 25 patients (60.98%) but poor identification in seven (17.07%) and 11 (26.83%) patients, respectively. With respect to venous

Table 1. Demographic and Clinical Characteristics of the Patients with Cerebral Vascular Lesions[a]

	AVM	dAVF	Total
Numbers	32	9	41
Gender			
Male	19	7	26
Female	13	2	15
Mean age, y	35.7 ± 14.5	56.7 ± 16.0	41.7 ± 18.4
Initial Diagnosis[b]	10	7	17 (41.46)
Follow-up[c]	22	2	24 (58.54)
Complete Obliteration	2	1	3 (7.32)

Abbreviations: AVM, arteriovenous malformation; dAVF, dural arteriovenous fistula.
[a]Values are expressed as mean $\pm$ SD, No., or No. (%).
[b]Examinations performed with unknown existing cerebral vascular lesions.
[c]Examinations performed after various endovascular or surgical treatments arteriovenous malformation.

drainage identification, including the routes of possible vein or sinus drainage, antegrade or retrograde patterns should both be taken into consideration. In the assessment of venous drainage, 4D-TRAK MRA was able to show almost all of the venous drainage in 38 patients (92.68%), while 3D TOF MRA only sufficiently visualized 16 patients (39.02%).

4.3. Interobserver Agreement

Table 3 summarizes the interobserver agreement between two readers. For diagnostic accuracy, 4D-TRAK MRA was excellent ($\kappa = 1.00$), while 3D TOF MRA was good ($\kappa = 0.793$). In the main arterial feeder assessment, 4D-TRAK was moderate ($\kappa = 0.592$) and good in 3D TOF MRA ($\kappa = 0.623$). For venous drainage, agreement of 4D-TRAK MRA was excellent ($\kappa = 1.00$), while 3D TOF MRA agreement was moderate ($\kappa = 0.572$).

4.4. Average Scores of Diagnostic Accuracy Index

The average scores were based on the 3-point grading system of diagnostic accuracy, arterial feeder and venous drainage. The comparison between the average scores of 4D-TRAK MRA and 3D TOF MRA is shown in Table 4. There was a statistically significant difference between 4D-TRAK MRA and 3D TOF MRA in terms of diagnostic accuracy in AVM (P = 0.006) and total group (summation of the AVM and dAVF, P = 0.002). For arterial identification, AVM, dAVF, and total group exhibited no significant differences. For venous drainage identification, 4D-TRAK MRA showed significant superiority to 3D TOF MRA in AVM (P < 0.0001) and total group (P < 0.0001). Figures 1 - 6 demonstrate the hemodynamic information, especially for drainage vein

identification, which was provided by 4D-TRAK MRA. However, 3D TOF MRA poorly showed venous drainage due to its "static" information.

5. Discussion

The most significant finding of this study is that 4D-TRAK MRA is able to provide nearly all valid diagnoses of AVM and dAVF. Furthermore, our study also shows that 4D-TRAK MRA is superior to 3D TOF MRA in diagnostic accuracy and venous drainage assessment. Regarding interobserver agreement, 4D-TRAK MRA showed excellent agreement in terms of diagnostic accuracy and venous drainage, as well as moderate agreement in arterial feeder identification. 3D TOF MRA presented good agreement in diagnostic accuracy and artery feeder assessment and moderate agreement in venous drainage. In short, compared with 3D TOF MRA, 4D-TRAK MRA was shown to be more reliable in diagnosing cerebral AVM and dAVF.

Our study shows that almost all vascular lesions and venous drainage patterns can be correctly evaluated by 4D-TRAK MRA, which is here shown to be superior to 3D TOF MRA (Tables 3 and 4). For the primary diagnosis of cerebral AVM and dAVF, or follow-up, the detection of early venous drainage is very important (23, 30). 4D-TRAK MRA provides both vascular anatomy and hemodynamic information, which are of great value in clinical assessments (17, 19), especially venous drainage patterns and possible fistula points. Comparatively, 3D TOF MRA only detected 39% of the venous drainage (Table 2). Slow flow fistulae or AVM may be easily missed (Figures 1 - 3) because 3D TOF MRA is a T1-weighted imaging technique for static vascular lesions (31). In addition, subacute thrombosis within a fistula vein may be misdiagnosed as a vascular lesion (32) because any

Table 2. Summary of Diagnostic Accuracy Scoring for Arterial Feeder and Venous Drainage on 4D-TRAK MRA and 3D TOF MRA

	Reader 1			Reader 2			Consensus Reading[a],[b]		
	Good	Equivocal	Poor	Good	Equivocal	Poor	Good	Equivocal	Poor
Diagnostic Accuracy									
4D-TRAK MRA	38	0	3	38	0	3	38 (92.68)	0	3 (7.32)
3D TOF MRA	30	2	9	26	4	11	26 (63.41)	6 (14.63)	9 (21.95)
Arterial Feeder									
4D-TRAK MRA	28	2	11	32	2	7	30 (73.17)	4 (9.76)	7 (17.07)
3D TOF MRA	26	1	14	24	4	13	25 (60.98)	5 (12.2)	11 (26.83)
Venous Drainage									
4D-TRAK MRA	38	0	3	38	0	3	38 (92.68)	0	3 (7.32)
3D TOF MRA	19	1	21	19	5	17	16 (39.02)	6 (14.63)	19 (46.34)

Abbreviations: 3D TOF MRA, three dimensional time-of-flight magnetic resonance angiography; 4D-TRAK MRA, 4D time-resolved angiography using keyhole magnetic resonance angiography.
[a] Values are expressed as No. (%).
[b] Disagreements between readers were reviewed by both readers to reach a consensus.

Table 3. Interobserver Agreement for Arteriovenous Malformation (AVMs) and Dural Arteriovenous Fistula (dAVFs) in 4D-TRAK MRA and 3D TOF MRA[a]

	Diagnostic Accuracy	Arterial Feeder	Venous Drainage
4D-TRAK MRA	1.000 (1.000 - 1.000)	0.592 (0.347 - 0.837)	1.000 (1.000 - 1.000)
3D TOF MRA	0.793 (0.605 - 0.981)	0.623 (0.411 - 0.835)	0.572 (0.366 - 0.778)

Abbreviations: 3D TOF MRA, three dimensional time-of-flight magnetic resonance angiography; 4D-TRAK MRA, 4D time-resolved angiography using keyhole magnetic resonance angiography.
[a] Interobserver agreement is between reader 1 and reader 2 and data were evaluated using Kappa statistics with 95% confidence intervals (CI) in parentheses.

Table 4. Average Diagnostic Accuracy Scores for AVM and dAVF by Means of 4D-TRAK MRA and 3D TOF MRA[a],[b]

	AVM	dAVF	All
Diagnostic Accuracy			
4D-TRAK MRA	1.88 (1.70 - 2.05)	1.78 (1.27 - 2.29)	1.85 (1.69 - 2.02)
3D TOF MRA	1.50 (1.23 - 1.77)	1.11 (0.30 - 1.92)	1.41 (1.15 - 1.68)
P value	0.006[c]	0.083	0.002[c]
Arterial Feeder			
4D-TRAK MRA	1.56 (1.27 - 1.85)	1.55 (1.00 - 2.11)	1.55 (1.32 - 1.81)
3D TOF MRA	1.41 (1.09 - 1.72)	1.11 (0.40 - 1.82)	1.34 (1.06 - 1.62)
P value	0.248	0.102	0.073
Venous Drainage			
4D-TRAK MRA	1.88 (1.70 - 2.05)	1.78 (1.27 - 2.29)	1.85 (1.69 - 2.02)
3D TOF MRA	0.87 (0.55 - 1.20)	1.11 (0.30 - 1.92)	0.93 (0.63 - 1.22)
P value	< 0.001[c]	0.083	< 0.001[c]

Abbreviations: AVM, arteriovenous malformation; dAVF, dural arteriovenous fistula; 3D TOF MRA, three dimensional time-of-flight magnetic resonance angiography; 4DTRAK MRA, 4D time-resolved angiography using keyhole magnetic resonance angiography.
[a] Average scores of diagnostic accuracy are the mean results of consensus reading according to a 3-point grading system.
[b] Data are presented as average score with the 95% CIs in parentheses.
[c] P value < 0.05 indicated statistical significance.
[c] P value < 0.05 indicated statistical significance.

high signal intensity on T1 weighted image could be easily presented on 3D TOF MRA (2, 33).

3D TOF MRA is a technique that mainly depends on the flow and movement of protons in the blood through the
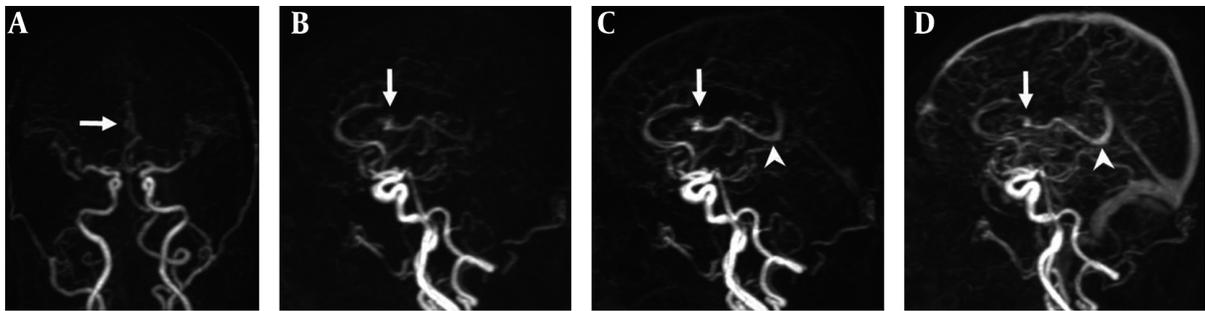
Figure 1. A 47-year-old man with a small AVM in the right lateral ventricle. A, Coronal TR-MRA shows the right lateral ventricle AVM with a nidus (arrow) supplied by a branch of the right anterior cerebral artery; B, Sagittal early; C, Late arterial; D, Venous phase TR-MRA images show the nidus (arrow) in the right lateral ventricle. Deep venous drainage occurs via an internal cerebral vein (arrow head) in the straight sinus.
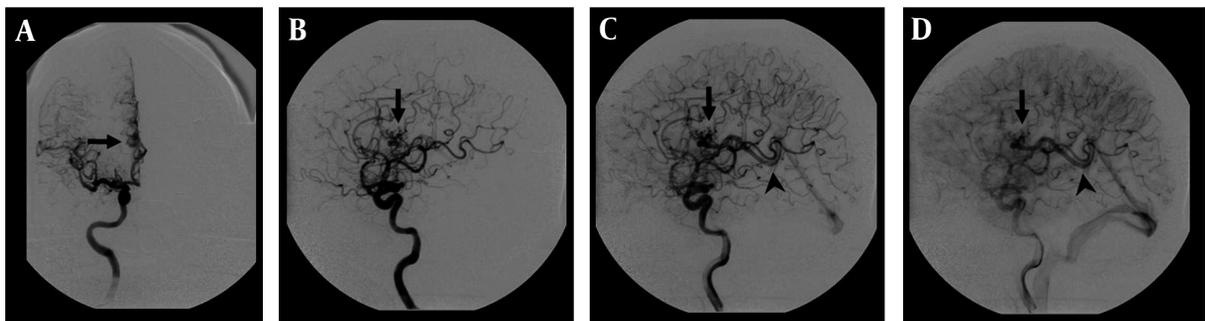

Figure 2. DSA examination of the AVM shown in Figure 1. A, Corresponding anteroposterior projection of injection into the right internal carotid artery, showing an AVM nidus (arrow) supplied by a branch of the right anterior cerebral artery; B, Early; and C, Late arterial; D, Venous phase lateral projections show the AVM nidus (arrow) and deep venous drainage occurs via an internal cerebral vein (arrow head) in the straight sinus.
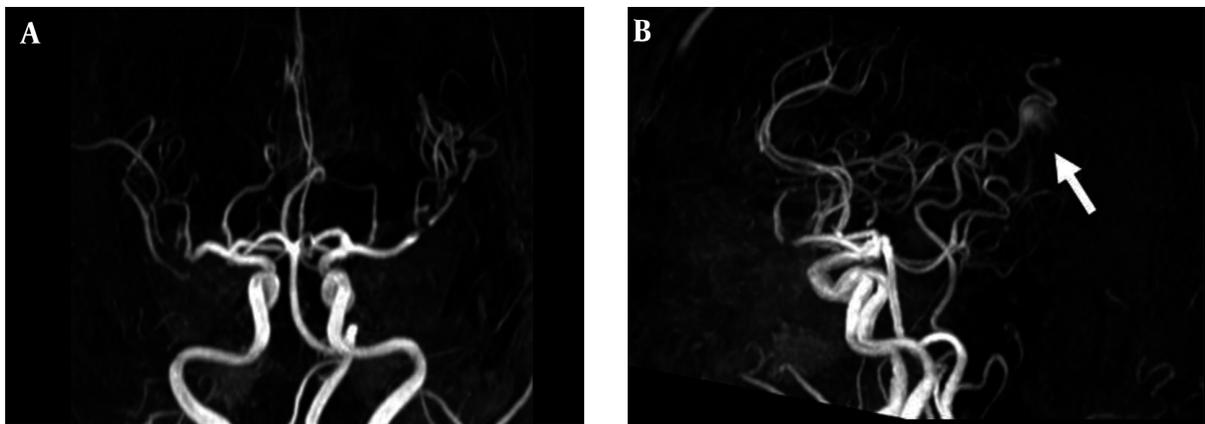
Figure 3. 3D TOF MRA of the AVM shown in Figure 1. A, Coronal; B, Sagittal views show no AVM nidus can be identified due to lack of venous phase information. A high signal intensity (arrow) resulting from flow artifacts of the great cerebral vein might be misdiagnosed as a vascular lesion.

imaging plane with a spoiled gradient echo, high flip angle and short TR. The image obtains relaxed inflowing blood as a high signal intensity under a saturated static magnetization background (1, 2, 27). The final images are reconstructed by MIP with rotation. Thus, vascular anatomy can be shown without contrast medium injection, eliminating the possibility of contrast medium allergic reactions or nephrogenic systemic fibrosis (NSF). Research in the re-
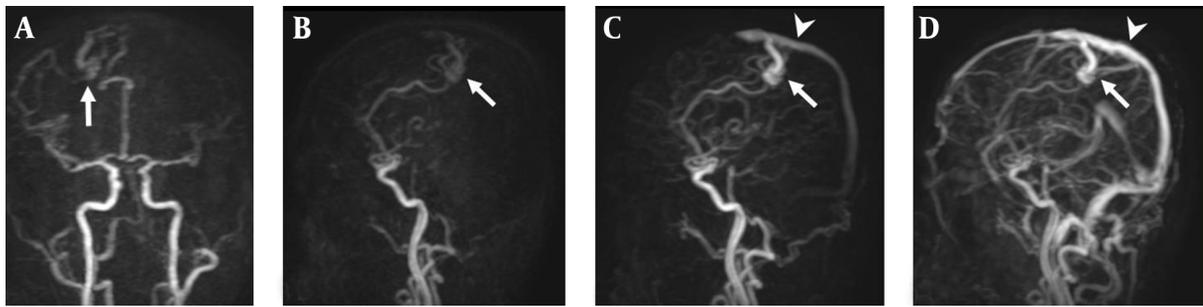
Figure 4. A 38-year-old man with right parietal lobe AVM. A, Coronal TR-MRA shows the right parietal AVM with a nidus (arrow) supplied by branches deriving from the right anterior and middle cerebral arteries; B, Sagittal early; C, Late arterial; D, Venous phase TR-MRA images show the AVM nidus (arrow) in the right parietal lobe. Superficial and venous drainage occurs via a dilated cortical vein in the superior sagittal sinus (arrow head).
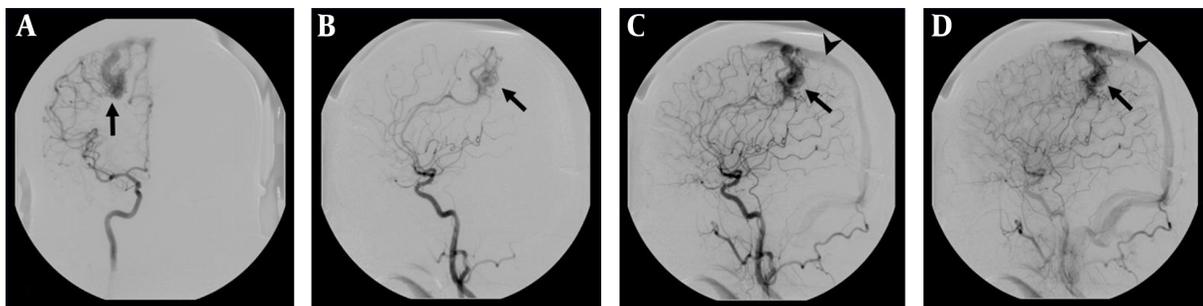
Figure 5. DSA examination of the AVM shown in Figure 4. A, The AVM is confirmed by the anteroposterior projection upon injection into the right internal carotid artery, which shows a vascular nidus (arrow) supplied by branches deriving from the right anterior and middle cerebral arteries. B, Early C, Late arterial; D, Venous phase lateral projections show the AVM nidus (arrow) and venous drainage occurs via a dilated cortical vein in the superior sagittal sinus (arrow head).
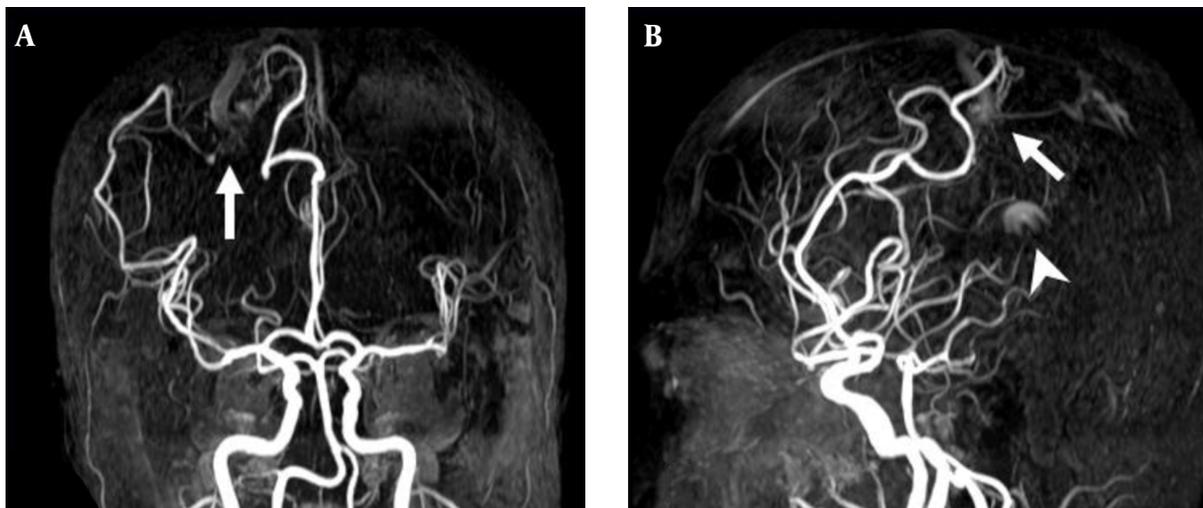
Figure 6. 3D TOF MRA of the AVM shown in Figure 4. A, Coronal; B, Sagittal views also reveal a focal hyperintense nidus (arrow) in the right parietal region supplied by branches deriving from right anterior and middle cerebral arteries. However, the venous drainage cannot be confirmed due to lack of venous phase information. In addition, a high signal intensity (arrow head) resulting from flow artifacts of the great cerebral vein is visualized.

cent years has shown that 3D TOF MRA can be regarded as a valuable tool for the initial diagnosis of dAVF and AVM

(31, 32, 34). They suggested abnormal hyperintensity on the images of 3D TOF MRA, which can provide the diagnosis of a possible fistula point or nidus formation. However, there are still some important shortcomings, including the following: the slow flow fistula may be missed, the possible subacute thrombosis within the fistula vein may show hyperintensity in complete occluded dAVF, and this may be misdiagnosed as fistula flow in follow-up images after treatment (27). Furthermore, dAVF with retrograde venous flow into the cortical veins may show a large portion of hyperintensity that may obscure the true fistula point or the location of a possible feeding artery. In addition, for primary diagnosis or follow-up of AVM and dAVF, identification of the drainage vein is very important (35-37). Thus, lack of hemodynamic information and venous phase information constitute the other drawback of this sequence. For these reasons, although the 3D TOF MRA is a useful method in the initial diagnosis of dAVF and AVMs, lack of dynamic information is a major shortcoming.

The interobserver agreement in 4D-TRAK MRA showed excellent agreement in lesion diagnosis and venous drainage assessment. Although the spatial resolution of 3D TOF MRA may sometimes be better than that of 4D-TRAK MRA (17), it is still not good enough for AVM nidus or fistula point identification. In other words, slow flow fistulae may be missed, and any hyperintensity may cause false interpretations of 3D TOF MRA. For this reason, the confidence of lesion depiction was lower, as was the interobserver agreement. With regard to the arterial feeder, neither interobserver agreement was excellent. We know that arterial feeders and even the main feeder to vascular lesions can be quite small in size. The relative poor spatial resolution may be the other factor causing artery assessment to be less consentient in 3D TOF MRA and even in 4D-TRAK MRA among readers with different diagnostic experiences (36). In addition, the capacity of traditional DSA in showing additional small feeders is due to its direct determination of the origin of the arterial feeders by injecting contrast medium into the four supra-aortic vessels, one by one, simply visualizing the nidus or fistula site. As a result, further advances in MRA techniques to improve spatial resolution are key points to be worked out in the future (30).

Although the diagnostic value and major arterial feeder identification of 3D TOF MRA have gained a certain reliability in current clinical use (31, 32), vessels with lower flows or smaller sizes may be still easily overlooked (27, 32). Furthermore, in some of our cases, the possible subacute thrombosis within fistula veins showing hyperintensity in completely occluded dAVF may be regarded as a residual fistula flow (38). Most importantly, without venous phase image for drainage vein assessment, the diagnostic accu-

racy of 3D TOF MRA is still far from equal to DSA, which requires the gold standard for characterization of AVM and dAVF (34). Comparatively, the higher diagnostic accuracy and venous drainage pattern recognized by the sequential arterial and venous phase images of 4D-TRAK MRA makes it far superior to 3D TOF MRA. Therefore, 4D-TRAK MRA is undoubtedly a more reliable tool in diagnosing cerebral AVM and dAVF.

The 4D-TRAK MRA acquired using CENTRA keyhole imaging, a parallel imaging technique and a multiphase acquisition technique, enables a rapid sequential analysis of arteries, capillaries and veins and facilitates the identification of early venous filling or retrograde flow in volumetric studies (16). The special k-space sampling is mainly divided into two regions: the centrally located k-space, which contributes to image contrast information by more frequent sampling, and the peripherally located regions, which provide high spatial resolution, true acceleration of the sequence acquisition time and fewer observed motion artifacts (19). Therefore, it can provide sequential arterial and venous phase images for venous drainage evaluation. From the results of our study, the definite lesion location, size, arterial feeder, and venous drainage all had good specificity in diagnosis. This means that the basic Spetzler-Martin grading of AVM (39), diagnosed by the nidus and venous drainage, and Borden-Shucart grading system of dAVF (40), mainly identified by the drainage vein, can be mostly diagnosed on 4D-TRAK MRA. Thus, with the aid of 4D-TRAK MRA, sufficient information for clinical therapeutic decision-making and planning can be obtained (30, 37, 41-43). Furthermore, this MR sequence requires only 1 minute for acquisition, while conventional DSA requires at least 30 minutes for the whole procedure. Therefore, 4D-TRAK MRA might be a good screening method for people with high clinical suspicions of AVM or dAVF. In short, 4D-TRAK MRA may reduce the necessity of performing conventional DSA for initial diagnosis or post-treatment follow-up in the future.

In our study, we observed that the vascular lesions that could not be correctly diagnosed on 4D-TRAK MRA were mostly small or those with extremely slow flows. This is because the specificity of CENTRA keyhole places emphasis on contrast data (central k-space) rather than on spatial resolution data (peripheral k-space), representing a trade-off in clinical practice between spatial resolution and temporal resolution. Consequently, the small residual nidus or extremely slow flow may cause some difficulties in identification, and traditional DSA may be the only choice for these small lesions. In other words, 4D-TRAK MRA can identify major arterial feeders but may overlook the small ones. Additionally, we also observed that there were identical results on 3D TOF MRA in three parameters of the dAVF

assessment (Table 4). The most reasonable explanation is that vascular lesions with prominent and fast flow venous drainage detected by 3D TOF MRA may be regarded as an early drainage vein. Furthermore, observing early drainage veins indicates a higher possibility of dAVF presence. Therefore, if the drainage vein is not identified, we will not be able to make the diagnosis.

The present study is not without limitations. First, no control group of patients without vascular lesion was established, so observer bias of the reviewers is present. Second, the time interval between MRA examination and conventional DSA may have caused some unpredictable differences between the two imaging modalities, even though the recruited patient population underwent two examinations within one month. Finally, the number of subjects in this study was small, consisting of only 41 patients in total. Subdividing these patients into groups such as AVM vs. dAVF and initial diagnosis vs. follow-up makes the small sample size an even bigger issue. Thus, further studies with larger numbers of patients to confirm the superior clinical results of 4D-TRAK MRA over 3D TOF MRA is needed.

In conclusion, although DSA is still the gold standard (43) in the diagnosis of cerebral AVM and dAVF, several different less invasive MRA sequences have gained clinical importance in the recent years. TR-MRA provides sequential arterial and venous phase images, making it superior to 3D TOF MRA in diagnostic accuracy. Our results suggest that TR-MRA seems to be a more reliable modality in the identification of cerebral AVM and dAVF.

References

1. Wheaton AJ, Miyazaki M. Non-contrast enhanced MR angiography: physical principles. *J Magn Reson Imaging.* 2012;**36**(2):286–304. doi: 10.1002/jmri.23641. [PubMed: 22807222].

2. Lim RP, Shapiro M, Wang EY, Law M, Babb JS, Rueff LE, et al. 3D time-resolved MR angiography (MRA) of the carotid arteries with time-resolved imaging with stochastic trajectories: comparison with 3D contrast-enhanced Bolus-Chase MRA and 3D time-of-flight MRA. *AJNR Am J Neuroradiol.* 2008;**29**(10):1847–54. doi: 10.3174/ajnr.A1252. [PubMed: 18768727].

3. Gupta V, Chugh M, Walia BS, Vaishya S, Jha AN. Use of CT angiography for anatomic localization of arteriovenous malformation Nidal components. *AJNR Am J Neuroradiol.* 2008;**29**(10):1837–40. doi: 10.3174/ajnr.A1136. [PubMed: 18768733].

4. Willems PW, Taeshineetanakul P, Schenk B, Brouwer PA, Terbrugge KG, Krings T. The use of 4D-CTA in the diagnostic work-up of brain arteriovenous malformations. *Neuroradiology.* 2012;**54**(2):123–31. doi: 10.1007/s00234-011-0864-0. [PubMed: 21465177].

5. Nussel F, Wegmuller H, Huber P. Comparison of magnetic resonance angiography, magnetic resonance imaging and conventional angiography in cerebral arteriovenous malformation. *Neuroradiology.* 1991;**33**(1):56–61. [PubMed: 2027447].

6. Blackham KA, Passalacqua MA, Sandhu GS, Gilkeson RC, Griswold MA, Gulani V. Applications of time-resolved MR angiography. *AJR Am J Roentgenol.* 2011;**196**(5):W613–20. doi: 10.2214/AJR.10.4227. [PubMed: 21512053].

7. Bink A, Berkefeld J, Wagner M, You SJ, Ackermann H, Lorenz MW, et al. Detection and grading of dAVF: prospects and limitations of 3T MRI. *Eur Radiol.* 2012;**22**(2):429–38. doi: 10.1007/s00330-011-2268-2. [PubMed: 21932162].

8. Pelz DM. Complication rates of DSA and conventional film cerebral angiography. *Radiology.* 1992;**185**(3):908. doi: 10.1148/radiology.185.3.1438785. [PubMed: 1438785].

9. Thiex R, Norbash AM, Frerichs KU. The safety of dedicated-team catheter-based diagnostic cerebral angiography in the era of advanced noninvasive imaging. *AJNR Am J Neuroradiol.* 2010;**31**(2):230–4. doi: 10.3174/ajnr.A1803. [PubMed: 19779004].

10. Bash S, Villablanca JP, Jahan R, Duckwiler G, Tillis M, Kidwell C, et al. Intracranial vascular stenosis and occlusive disease: evaluation with CT angiography, MR angiography, and digital subtraction angiography. *AJNR Am J Neuroradiol.* 2005;**26**(5):1012–21. [PubMed: 15891154].

11. American College of Radiology. . Manual on Contrast Media. 2012

12. Unlu E, Temizoz O, Albayram S, Genchellac H, Hamamcioglu MK, Kurt I, et al. Contrast-enhanced MR 3D angiography in the assessment of brain AVMs. *Eur J Radiol.* 2006;**60**(3):367–78. doi: 10.1016/j.ejrad.2006.08.007. [PubMed: 16965882].

13. Grist TM, Mistretta CA, Strother CM, Turski PA. Time-resolved angiography: Past, present, and future. *J Magn Reson Imaging.* 2012;**36**(6):1273–86. doi: 10.1002/jmri.23646. [PubMed: 22566099].

14. Carroll TJ. The emergence of time-resolved contrast-enhanced MR imaging for intracranial angiography. *AJNR Am J Neuroradiol.* 2002;**23**(3):346–8. [PubMed: 11900996].

15. Parmar H, Ivancevic MK, Dudek N, Gandhi D, Mukherji SK. Dynamic MRA with four-dimensional time-resolved angiography using keyhole at 3 tesla in head and neck vascular lesions. *J Neuroophthalmol.* 2009;**29**(2):119–27. doi: 10.1097/WNO.0b013e3181a58c20. [PubMed: 19491635].

16. Hadizadeh DR, Gieseke J, Beck G, Geerts L, Kukuk GM, Bostrom A, et al. View-sharing in keyhole imaging: Partially compressed central k-space acquisition in time-resolved MRA at 3.0 T. *Eur J Radiol.* 2011;**80**(2):400–6. doi: 10.1016/j.ejrad.2010.04.020. [PubMed: 20447790].

17. Krings T, Hans F. New developments in MRA: time-resolved MRA. *Neuroradiology.* 2004;**46 Suppl 2**:s214–22. doi: 10.1007/s00234-004-1332-x. [PubMed: 15645155].

18. Riffel P, Haneder S, Attenberger UI, Brade J, Schoenberg SO, Michaely HJ. Combined large field-of-view MRA and time-resolved MRA of the lower extremities: impact of acquisition order on image quality. *Eur J Radiol.* 2012;**81**(10):2754–8. doi: 10.1016/j.ejrad.2011.12.003. [PubMed: 22185939].

19. Willinek WA, Hadizadeh DR, von Falkenhausen M, Urbach H, Hoogeveen R, Schild HH, et al. 4D time-resolved MR angiography with keyhole (4D-TRAK): more than 60 times accelerated MRA using a combination of CENTRA, keyhole, and SENSE at 3.0T. *J Magn Reson Imaging.* 2008;**27**(6):1455–60. doi: 10.1002/jmri.21354. [PubMed: 18504736].

20. Song T, Laine AF, Chen Q, Rusinek H, Bokacheva L, Lim RP, et al. Optimal k-space sampling for dynamic contrast-enhanced MRI with an application to MR renography. *Magn Reson Med.* 2009;**61**(5):1242–8. doi: 10.1002/mrm.21901. [PubMed: 19230014].

21. Gauvrit JY, Law M, Xu J, Carson R, Sunenshine P, Chen Q. Time-resolved MR angiography: optimal parallel imaging method. *AJNR Am J Neuroradiol.* 2007;**28**(5):835–8. [PubMed: 17494652].

22. Horie T, Honda M, Okumura Y, Usui K, Kaneko A, Muro I, et al. [Basic examination of CEMRA with 4D time-resolved angiography using keyhole (4D-TRAK) in 3T pelvic region]. *Nihon Hoshasen Gijutsu Gakkai Zasshi.* 2008;**64**(12):1532–9. [PubMed: 19151522].

23. Farb RI, Agid R, Willinsky RA, Johnstone DM, Terbrugge KG. Cranial dural arteriovenous fistula: diagnosis and classification with time-resolved MR angiography at 3T. *AJNR Am J Neuroradiol.* 2009;**30**(8):1546–51. doi: 10.3174/ajnr.A1646. [PubMed: 19474117].

24. Higashihara H, Osuga K, Ueguchi T, Onishi H, Tanaka H, Maeda N, et al. Usefulness of contrast-enhanced three-dimensional MR angiography using time-resolved imaging of contrast kinetics applied to description of Extracranial Arteriovenous Malformations: initial experience. *Eur J Radiol.* 2012;**81**(6):1134–9. doi: 10.1016/j.ejrad.2011.03.040. [PubMed: 21474262].

25. Hadizadeh DR, Kukuk GM, Steck DT, Gieseke J, Urbach H, Tschampa HJ, et al. Noninvasive evaluation of cerebral arteriovenous malformations by 4D-MRA for preoperative planning and postoperative follow-up in 56 patients: comparison with DSA and intraoperative findings. *AJNR Am J Neuroradiol.* 2012;**33**(6):1095–101. doi: 10.3174/ajnr.A2921. [PubMed: 22300925].

26. Nael K, Villablanca JP, Saleh R, Pope W, Nael A, Laub G, et al. Contrast-enhanced MR angiography at 3T in the evaluation of intracranial aneurysms: a comparison with time-of-flight MR angiography. *AJNR Am J Neuroradiol.* 2006;**27**(10):2118–21. [PubMed: 17110679].

27. Buis DR, Bot JC, Barkhof F, Knol DL, Lagerwaard FJ, Slotman BJ, et al. The predictive value of 3D time-of-flight MR angiography in assessment of brain arteriovenous malformation obliteration after radiosurgery. *AJNR Am J Neuroradiol.* 2012;**33**(2):232–8. doi: 10.3174/ajnr.A2744. [PubMed: 22095967].

28. Wu Q, Li MH. A comparison of 4D time-resolved MRA with keyhole and 3D time-of-flight MRA at 3.0 T for the evaluation of cerebral aneurysms. *BMC Neurol.* 2012;**12**:50. doi: 10.1186/1471-2377-12-50. [PubMed: 22784396].

29. Gailloud P. Endovascular treatment of cerebral arteriovenous malformations. *Tech Vasc Interv Radiol.* 2005;**8**(3):118–28. doi: 10.1053/j.tvir.2005.10.003. [PubMed: 16376787].

30. Nishimura S, Hirai T, Sasao A, Kitajima M, Morioka M, Kai Y, et al. Evaluation of dural arteriovenous fistulas with 4D contrast-enhanced MR angiography at 3T. *AJNR Am J Neuroradiol.* 2010;**31**(1):80–5. doi: 10.3174/ajnr.A1898. [PubMed: 19833802].

31. Yu S, Yan L, Yao Y, Wang S, Yang M, Wang B, et al. Noncontrast dynamic MRA in intracranial arteriovenous malformation (AVM), comparison with time of flight (TOF) and digital subtraction angiography (DSA). *Magn Reson Imaging.* 2012;**30**(6):869–77. doi: 10.1016/j.mri.2012.02.027. [PubMed: 22521994].

32. Noguchi K, Melhem ER, Kanazawa T, Kubo M, Kuwayama N, Seto H. Intracranial dural arteriovenous fistulas: evaluation with combined 3D time-of-flight MR angiography and MR digital subtraction angiography. *AJR Am J Roentgenol.* 2004;**182**(1):183–90. doi: 10.2214/ajr.182.1.1820183. [PubMed: 14684537].

33. Deutschmann HA, Augustin M, Simbrunner J, Unger B, Schoellnast H, Fritz GA, et al. Diagnostic accuracy of 3D time-of-flight MR angiography compared with digital subtraction angiography for follow-up of coiled intracranial aneurysms: influence of aneurysm size. *AJNR Am J Neuroradiol.* 2007;**28**(4):628–34. [PubMed: 17416811].

34. Heidenreich JO, Schilling AM, Unterharnscheidt F, Stendel R, Hartlieb S, Wacker FK, et al. Assessment of 3D-TOF-MRA at 3.0 Tesla in the characterization of the angioarchitecture of cerebral arteriovenous malformations: a preliminary study. *Acta Radiol.* 2007;**48**(6):678–86. doi: 10.1080/02841850701326958. [PubMed: 17611878].

35. Oleaga L, Dalal SS, Weigele JB, Hurst RW, Lee J, Voorhees A, et al. The role of time-resolved 3D contrast-enhanced MR angiography in the assessment and grading of cerebral arteriovenous malformations. *Eur J Radiol.* 2010;**74**(3):e117–21. doi: 10.1016/j.ejrad.2009.04.063. [PubMed: 19467814].

36. Machet A, Portefaix C, Kadziolka K, Robin G, Lanoix O, Pierot L. Brain arteriovenous malformation diagnosis: value of time-resolved contrast-enhanced MR angiography at 3.0T compared to DSA. *Neuroradiology.* 2012;**54**(10):1099–108. doi: 10.1007/s00234-012-1024-x. [PubMed: 22407410].

37. Klisch J, Strecker R, Hennig J, Schumacher M. Time-resolved projection MRA: clinical application in intracranial vascular malformations. *Neuroradiology.* 2000;**42**(2):104–7. [PubMed: 10663484].

38. Meckel S, Maier M, Ruiz DS, Yilmaz H, Scheffler K, Radue EW, et al. MR angiography of dural arteriovenous fistulas: diagnosis and follow-up after treatment using a time-resolved 3D contrast-enhanced technique. *AJNR Am J Neuroradiol.* 2007;**28**(5):877–84. [PubMed: 17494662].

39. Altay T. Management of arteriovenous malformations related to Spetzler-Martin grading system. *J Neurol Surg A Cent Eur Neurosurg.* 2012;**73**(5):307–19. doi: 10.1055/s-0032-1315791. [PubMed: 22773439].

40. Zipfel GJ, Shah MN, Refai D, Dacey RJ, Derdeyn CP. Cranial dural arteriovenous fistulas: modification of angiographic classification scales based on new natural history data. *Neurosurg Focus.* 2009;**26**(5):E14. doi: 10.3171/2009.2.FOCUS0928. [PubMed: 19408992].

41. Ali S, Cashen TA, Carroll TJ, McComb E, Muzaffar M, Shaibani A, et al. Time-resolved spinal MR angiography: initial clinical experience in the evaluation of spinal arteriovenous shunts. *AJNR Am J Neuroradiol.* 2007;**28**(9):1806–10. doi: 10.3174/ajnr.A0639. [PubMed: 17885246].

42. Taschner CA, Gieseke J, Le Thuc V, Rachdi H, Reyns N, Gauvrit JY, et al. Intracranial arteriovenous malformation: time-resolved contrast-enhanced MR angiography with combination of parallel imaging, keyhole acquisition, and k-space sampling techniques at 1.5 T. *Radiology.* 2008;**246**(3):871–9. doi: 10.1148/radiol.2463070293. [PubMed: 18195381].

43. Nishimura S, Hirai T, Shigematsu Y, Kitajima M, Morioka M, Kai Y, et al. Evaluation of brain and head and neck tumors with 4D contrast-enhanced MR angiography at 3T. *AJNR Am J Neuroradiol.* 2012;**33**(3):445–8. doi: 10.3174/ajnr.A2819. [PubMed: 22116118].